

## Automated Detection of Arteriovenous Crossing Phenomenon on Retinal Images

Yuji Hatanaka<sup>1</sup>, Chisako Muramatsu<sup>2</sup>, Takeshi Hara<sup>2</sup>, Hiroshi Fujita<sup>2</sup>

<sup>1</sup> School of Engineering, The University of Shiga Prefecture, Shiga 522-8533, Japan

<sup>2</sup> Graduate School of Medicine, Gifu University, Gifu 501-1194, Japan

hatanaka.y@usp.ac.jp, chisa@fjt.info.gifu-u.ac.jp, hara@info.gifu-u.ac.jp, fujita@fjt.info.gifu-u.ac.jp

**ABSTRACT:** Arteriosclerosis is one cause of acquired blindness. Retinal fundus image examination is useful for early detection of arteriosclerosis. In order to diagnose the presence of arteriosclerosis, the physicians find the silver-wire arteries, the copper-wire arteries and arteriovenous crossing phenomenon on retinal fundus images. The focus of this study was to develop the automated detection method of the arteriovenous crossing phenomenon on the retinal images. The blood vessel regions were detected by using a double ring filter, and the cross sections of artery and vein were detected by using a ring filter. The center of that ring was an interest point, and that point was determined as a cross section when there were over four blood vessel segments on that ring. And two blood vessels gone through on the ring were classified into artery and vein by using the pixel values on red and blue component image. Finally,  $V_2$ -to- $V_1$  ratio was measured for recognition of abnormalities.  $V_1$  was the venous diameter far from the blood vessel cross section, and  $V_2$  was the venous diameter near from the blood vessel cross section. The cross section with  $V_2$ -to- $V_1$  ratio over 0.8 was experimentally determined as abnormality. Twenty four images, including 27 abnormalities and 54 normal cross sections, were used for preliminary evaluation of the proposed method. The proposed method was detected 73% of cross sections when the 2.8 sections per image were mis-detected. And, 59% of abnormalities were detected by measurement of  $V_1$ -to- $V_2$  ratio when the 1.7 sections per image were mis-detected.

**KEYWORDS:** Arteriosclerosis, Hypertensive retinopathy, Retinal Fundus image, Arteriovenous crossing phenomenon, Image analysis, Computer-aided diagnosis

### I. INTRODUCTION

The fundus is examined selectively in the diagnosis performed by physicians as part of a specific health checkup scheme initiated in Japan in April 2008. Thus, the numbers of retinal examinations have been increased. Computer-aided diagnosis (CAD) systems, developed for analyzing retinal fundus images, can assist in reducing the workload of ophthalmologists and improving the screening accuracy. Thus, we have been developing a CAD system for analyzing retinal fundus images [1-13]. Our CAD system was targeted for three diseases, hypertensive retinopathy [1-5], diabetic retinopathy [6-8] and glaucoma [9-13]. Using Scheie classification, hypertensive retinopathy is divided into two main categories, retinopathy and arteriosclerosis. Arteriosclerosis was graded by silver-wire artery, copper-wire artery and arteriovenous crossing phenomenon (AVCP) [14]. If the venous diameter  $V_2$  near the cross section of the artery and the vein was narrow than the venous diameter  $V_1$

far from the cross section, the section was determined as AVCP (as shown in Figure 1). But, to detect AVCP automatically was very difficult, and automatic AVCP detection was no reported. Thus, this study was designed to develop an automated method for detecting AVCP on retinal fundus images.

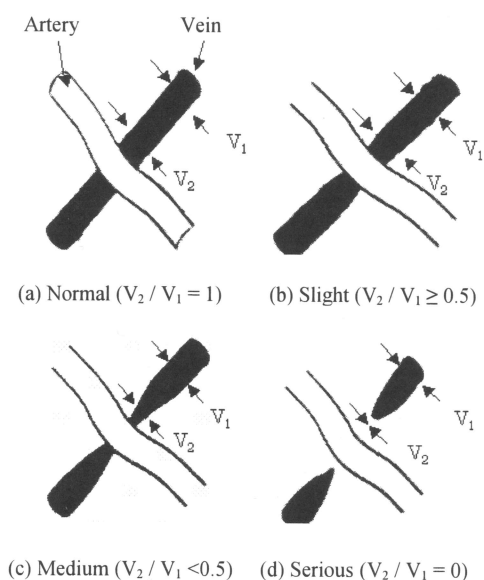


Figure 1. Grades of arteriovenous crossing point.

### II. METHODS

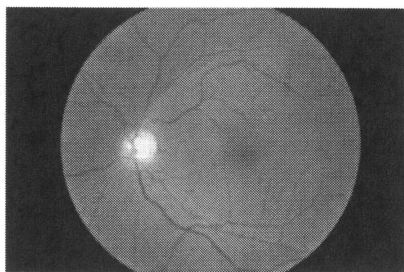
Retinal fundus images were captured using a fundus camera (the nonmyd 7, Kowa Company, Ltd., Tokyo, Japan). The photographic angle of the fundus camera was set to 45 degrees. The retinal fundus images were obtained with an array size of  $3008 \times 2000$  pixels and 24-bit color.

Next, the blood vessels (BV) regions were detected. Much research has been conducted on automated BVs detection on retinal images [1-4, 14-17]. They include the methods using matched filters [14], differential filters [15], region growing [16] and Gabor wavelets [17]. We also developed BVs detection methods using a double ring filter [1, 2] and black top hat transformation [3, 4]. A double ring filter was used for BVs detection in this study. Figure 2 shows a result of BVs detection by using a double ring filter. The optic disc region was then detected by using p-tile

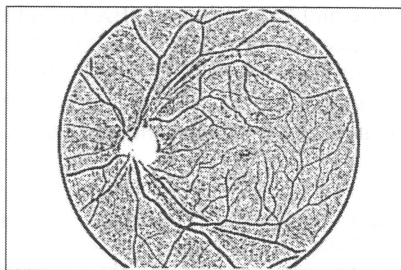
technique of the histogram with green component of color image.

The major BVs used for the AVCP detection usually run from the optic disc to the upper and lower temporal regions. In order to select such BVs, a vessel-range mask was superimposed to the images for including vessels that were inside this mask. The vessel-range mask was created based on the BVs in the 24 cases by centering the optic discs as shown in Figure 3. To detect the cross sections of the artery and the vein, a ring filter was determined (as shown in Figure 4). If over 4 BVs were existed on the ring, the interest point was determined as the cross section. But this ring filter misdetected many false positives like Figure 5 (b), and they were reduced by using contrasts between the pixel value on interest pixel and pixel value on the position far from there on green and blue components of color image.

The artery and the vein were classified by using pixel values on the ring (as shown in Figure 6). The four pixel

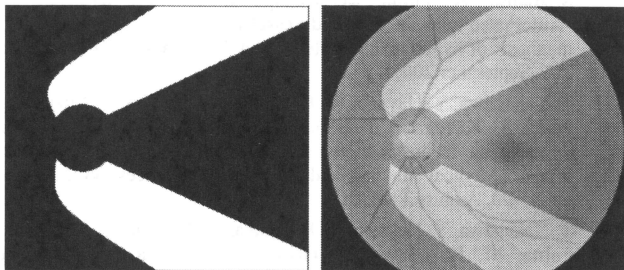


(a) Original retinal fundus image



(b) Result of the blood vessels detection.

Figure 2. Detection of blood vessels by using double ring filter.

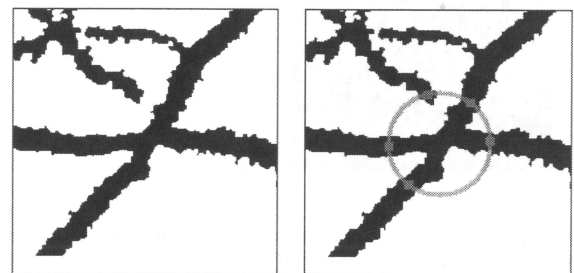


(a)

(b)

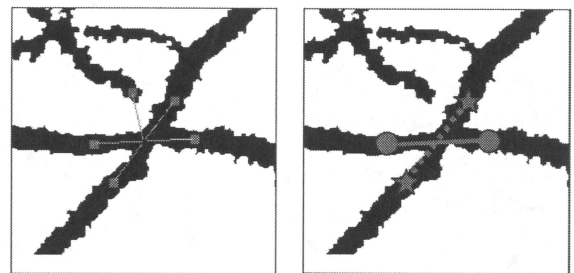
Figure 3. The vessel-range mask. (a) The range of the arteriovenous crossing phenomenon locations determined by superimposing the optic disc centers of the 24 cases. (b) The searching area was determined by superimposing the range.

values of 4 BV points on the ring were ranked on the red and green components. The ranking values were summed, and that sum and that opposite sum of the ring were summed. The vein was darker than the artery in the color image, thus the BV with smaller sum was classified as the vein. Then,  $V_1$  and  $V_2$  were then determined for detection of the AVCP. The vein on the ring was determined as the center of the ring on the vein was determined as the position  $P_2$  (as shown in Figure 7).  $V_1$  was the average venous diameter between  $P_1$  and  $P_2$ , and  $V_2$  was the minimum venous diameter between  $P_2$  and the interest point. Finally, the interesting point was experimentally determined as AVCP when the  $V_2$ -to- $V_1$  ( $V_2 / V_1$ ) ratio was under 0.8.



(a)

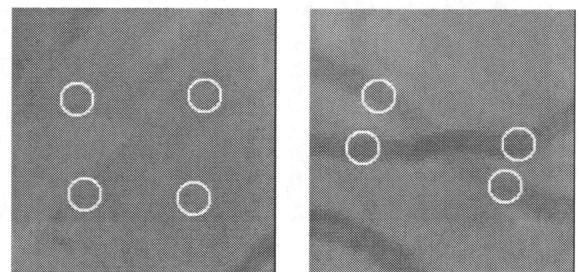
(b)



(c)

(d)

Figure 4. Using a ring filter, the cross sections of artery and vein was detected. (a) Result of blood vessels detection. (b) The ring filter for searching the cross sections. Green line shows a ring filter, and red points show the positions crossing the blood vessel and a ring. (c) False blood vessels elimination. The blood vessels without the opposite blood vessel candidates of the ring were removed. Top and left blood vessel was removed in this case. (d) The cross section was detected by recognition of artery and vein pair.



(a) True AVCP

(b) False AVCP

Figure 5. The different pixel value of true AVCP and false one. White circles were misdetections as blood vessels in (b).

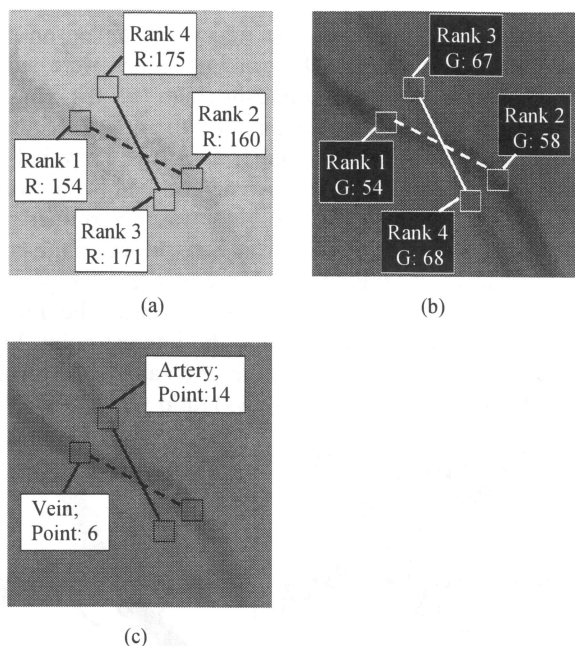


Figure 6. Classification of artery and vein. (a) The red pixel values on the ring, and their ranks in 4 points. (b) The green pixel values on the ring, and their ranks in 4 points. (c) The distinction points by the sum of the ranks on red and green components.

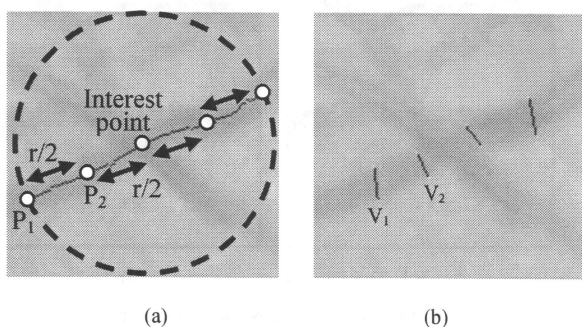


Figure 7. Determination of diameter  $V_1$  and  $V_2$ . (a) The vein on the ring was determined as the position  $P_1$ . The venous position on the ring with half radius of the ring filter was determined as the position  $P_2$ . " $r$ " is a radius of the ring. (b)  $V_1$  was the average venous diameter between  $P_1$  and  $P_2$ .  $V_2$  was the minimum venous diameter between  $P_2$  and the interest point.

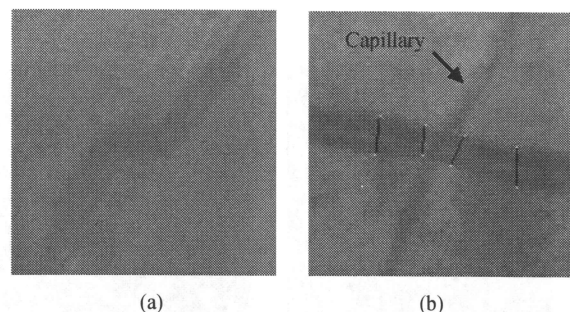


Figure 8. These cases are false. (a) The proposed method did not detect this cross section because this included artery wall reflection (which is called silver or cooper wire artery). (b) This cross section was mis-detected because this region includes the capillary crossed the fat main blood vessel.

### III. RESULTS AND DISCUSSION

Twenty four retinal fundus images, including 27 AVCP and 54 normal cross sections, were used to evaluate the proposed method for detection of AVCP preliminary. The proposed method was detected 73% (59 / 81) of BV cross sections including when the 2.8 (66/24) sections per image were mis-detected. And, 59% (16/27) of the sections with AVCP were detected by measurement of  $V_2 / V_1$  ratio when the 1.7 (41/24) sections per image were mis-detected.

The proposed method could not detect BV cross sections with low contrast of an artery (as shown in Figure 8 (a)) in this evaluation. Their arteriolar walls were reflected, thus detection of such arteries were very difficult. Moreover, proposed method would mis-detect the capillaries like Figure 8 (b), if it detects such arteries. We have been developing a BV tracking method from the optic disc for determination of artery-vein diameter ratio [5], thus the problem (like Figure 8 (b)) may be improved by using such a technique.

### IV. CONCLUSION

We proposed an automated AVCP detection method based on the vein diameter measurement near BV cross section. The preliminary result indicated the potential usefulness of this method for the automated BV crossing sections detection. But, the automated AVCP detection method needs to improve.

### ACKNOWLEDGMENT

This project is funded by the Grant-in-Aid for Young Scientists (B) from the Ministry of Education, Culture, Sports, Science and Technology (MEXT), and a grant for the Knowledge Cluster Gifu-Ogaki (KCGO), referred to as the "Robotics Advanced Medical Cluster," from the MEXT, Japan. The authors are grateful to their many co-workers from Gifu University, hospitals, and companies.

### REFERENCES

- [1] Y. Hatanaka, T. Nakagawa, Y. Hayashi, A. Aoyama, X. Zhou, T. Hara, H. Fujita, Y. Mizukusa, A. Fujita, and M. Kakogawa, "Automated detection algorithm for arteriolar narrowing on fundus images," Proc 27th Annual International Conf. IEEE Eng. Med. Biomed. Society, pp. #291, September 2005, doi: 10.1109/IEMBS.2005.1616400.
- [2] R. Takahashi, Y. Hatanaka, T. Nakagawa, Y. Hayashi, A. Aoyama, Y. Mizukusa, A. Fujita, M. Kakogawa, T. Hara, and H. Fujita, "Automated analysis of blood vessel intersections retinal images for diagnosis of hypertension," Med. Imag. Tech., vol. 24, no. 4, pp. 270-276, September 2006.
- [3] T. Nakagawa, Y. Hayashi, Y. Hatanaka, A. Aoyama, Y. Mizukusa, A. Fujita, M. Kakogawa, T. Hara, H. Fujita, and T. Yamamoto, "Three-dimensional reconstruction using a single two-dimensional retinal image," Medical Imaging and Information Sciences, Vol. 23, no. 2, pp. 85-90, August 2006.
- [4] T. Nakagawa, Y. Hayashi, Y. Hatanaka, A. Aoyama, Y. Mizukusa, A. Fujita, M. Kakogawa, T. Hara, H. Fujita, and T. Yamamoto, "Recognition of optic nerve head using blood-vessel-erased image and its application to production of simulated stereogram in computer-aided diagnosis system for retinal images," IEICE Trans. Info. and Sys., vol. E93-D, no.9, pp. 2397-2406, September, 2006.
- [5] C. Muramatsu, Y. Hatanaka, T. Iwase, and H. Fujita, "Automated detection and classification of major retinal vessels for determination

- of diameter ratio of arteries and veins," Proc. SPIE, vol. 7624, pp. 76240J-1-8, February 2010, doi: 10.1117/12.843898.
- [6] Y. Hatanaka, T. Nakagawa, Y. Hayashi, A. Fujita, M. Kakogawa, K. Kawase, T. Hara, and H. Fujita, "CAD scheme to detect hemorrhages and exudates in ocular fundus images," Proc. SPIE, vol. 6514, pp. 65142M-1-8, February 2007, doi: 10.1117/12.708367.
- [7] Y. Hatanaka, T. Nakagawa, Y. Hayashi, T. Hara, and H. Fujita, "Improvement of automated detection method of hemorrhages in fundus images," Proc 30th Annual International Conf. IEEE Eng. Med. Biomed. Society, pp. 5429-5432, August 2008, doi: 10.1109/IEEMBS.2008.4650442
- [8] M. Niemeijer, B. van Ginneken, M. J. Cree, A. Mizutani, G. Quellec, C. I. Sanchez, B. Zhang, R. Hornero, M. Lamard, C. Muramatsu, X. Wu, G. Cazuguel, J. You, A. Mayo, Q. Li, Y. Hatanaka, B. Cochener, C. Roux, F. Karray, M. Garcia, H. Fujita, and M. D. Abramoff, "Retinopathy online challenge: Automatic detection of microaneurysms in digital color fundus photographs," IEEE Trans. Med. Imag., vol. 29, no. 1, pp. 185-195, January 2010, doi: 10.1109/TMI.2009.2033909
- [9] C. Muramatsu, Y. Hayashi, A. Sawada, Y. Hatanaka, T. Hara, T. Yamamoto, and H. Fujita, "Detection of retinal nerve fiber layer defects on retinal fundus images for early diagnosis of glaucoma," J. Biomed. Optics, vol. 15, no. 1, pp.016021-1-7, January 2010, doi: 10.1117/12.863325.
- [10] C. Muramatsu, T. Nakagawa, A. Sawada, Y. Hatanaka, T. Hara, T. Yamamoto, and H. Fujita, "Automated segmentation of optic disc region on retinal fundus photographs: Comparison of contour modeling and pixel classification methods," Comp. Methods Prog. Biomed., in Press, doi: 10.1016/j.cmpb.2010.04.006.
- [11] Y. Hatanaka, A. Noudo, C. Muramatsu, A. Sawada, T. Hara, T. Yamamoto, and H. Fujita, "Automatic measurement of vertical cup-to-disc ratio on retinal fundus images," Medical Biometrics, LNCS, vol. 6165, pp. 54-72, June 2010, doi: 10.1007/978-3-642-13923-9\_7.
- [12] T. Nakagawa, T. Suzuki, Y. Hayashi, Y. Mizukusa, Y. Hatanaka, K. Ishida, T. Hara, H. Fujita, and T. Yamamoto, "Quantitative depth analysis of optic nerve head using stereo retinal fundus image pair," J. Biomed. Optics, vol. 13, no.6, pp. 064026(1-10), November 2008, doi: 10.1117/12.823869.
- [13] C. Muramatsu, T. Nakagawa, A. Sawada, Y. Hatanaka, T. Hara, T. Yamamoto, and H. Fujita, "Determination of cup and disc ratio of optical nerve head for diagnosis of glaucoma on stereo retinal fundus image pairs," Proc. SPIE, vol. 7260, pp. 72603L-1-8, February 2009.
- [14] H. G. Scheie, "Evaluation of ophthalmoscopic changes of hypertension and arteriolar sclerosis," A. M. A. Arch. Ophthalmol. Vol. 49, no. 2, pp. 117-38, February 1953.
- [15] A. Hoover, V. Kouznetsova, and M. Goldbaum, "Locating blood vessels in retinal images by piece-wise threshold probing of a matched filter response," IEEE Trans. Med. Imag. vol. 19, no. 3, pp 203-210, March 2000, doi: 10.1109/42.845178.
- [16] J. J. Staal, M. D. Abramoff, M. Niemeijer, M. A. Viergever, and B. van Ginneken, "Ridge based vessel segmentation in color images of the retina," IEEE Trans. Med. Imag., vol. 23, no. 4, pp. 501-509, April 2004, doi: 10.1109/TMI.2004.825627.
- [17] M. Himaga, D. Usher, and J. F. Boyce, "Accurate retinal blood vessel segmentation by using multi-resolution matched filtering and directional region growing." IEICE Trans. Info. Sys., vol. E87-D, no. 1, pp. 155-163, January 2004.
- [18] R. M. Rangayyan, F. J. Ayres, F. Oloumi, P. Eshghzadeh-Zanjani, "Detection of blood vessels in the retina with multiscale Gabor filters," J. Electron Imag., vol. 17, no. 2, pp.023018, April 2008, doi: 10.1117/12.803748.